

See discussions, stats, and author profiles for this publication at: <https://www.researchgate.net/publication/278695807>

# Development of an Integrated Oil Shale Refinery Process with Coal Gasification for Hydrogen Production

ARTICLE *in* INDUSTRIAL & ENGINEERING CHEMISTRY RESEARCH · DECEMBER 2014

Impact Factor: 2.59 · DOI: 10.1021/ie5024436

---

CITATIONS

4

---

READS

24

5 AUTHORS, INCLUDING:



[Yu Qian](#)

South China University of Technology

203 PUBLICATIONS 1,609 CITATIONS

SEE PROFILE



[Qingchun Yang](#)

South China University of Technology

9 PUBLICATIONS 44 CITATIONS

SEE PROFILE



[Huairong Zhou](#)

South China University of Technology

7 PUBLICATIONS 10 CITATIONS

SEE PROFILE

# Development of an Integrated Oil Shale Refinery Process with Coal Gasification for Hydrogen Production

Yu Qian, Qingchun Yang, Jun Zhang, Huairong Zhou, and Siyu Yang\*

School of Chemical Engineering, South China University of Technology, Guangzhou 510641, P. R. China

**ABSTRACT:** Exploration and exploitation of oil shale are of increasing interest to the countries with scarce oil reserves. Retorting technology is applied to produce shale oil. However, most of retorting processes waste detrital oil shale and the remaining gas, leading to low economic benefit. An integrated oil shale refinery process with coal gasification in supercritical water is proposed for better economic performance than the conventional retorting processes. In the proposed process, coal in shale mines is gasified in supercritical water to produce hydrogen. The hydrogen is used in the hydrogenation process to upgrade shale oil to diesel, naphtha, liquefied petroleum gas, etc. The detrital oil shale and remaining gas are burned to heat the gasification process. The proposed process is modeled and simulated for techno-economic analysis. The economic performance of the proposed process is compared with that of the conventional retorting process. Results show that the return on investment of the proposed process is 22.72%, much higher than the conventional one, 14.45%.

## 1. INTRODUCTION

The increasing demand of oil is in conflict with the shortage of oil supply, forcing many countries to seek alternative energy resources. Oil shale is now considered as one of the promising oil alternatives.<sup>1</sup> With soaring international petroleum price, many countries, especially China, Estonia, and Brazil, are making big efforts to develop efficient, environmental-friendly, and economical retorting techniques.<sup>2,3</sup>

Ex situ retorting and in situ retorting are the two major oil shale retorting technologies. In situ retorting is still under developing and will not be in large-scale operation for at least a decade.<sup>4</sup> The ex situ retorting technique has been successfully implemented in a Petrosix-type retort in Brazil, ATP-type retort in Australia, and Kiviter and Galoter-type retort in Estonia.<sup>5–7</sup> In China, Fushun-type retort, a self-developed ex situ retorting technique, is widely used.<sup>5,8</sup> However, this retorting technique suffers from relative poor economic performance.<sup>9</sup> A few studies<sup>8,10</sup> were proposed to use the detrital oil shale and ash to make building materials. This could reduce solid waste pollution. The oil shale retorting process with a building material production process is shown in Figure 1. This process

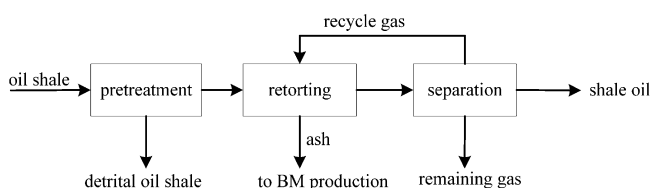


**Figure 1.** Schematic diagram of the OSR process.

is set as the benchmark in this paper. The oil shale is crushed and screened into particles with sizes in the required range. They are then heated up to near 525 °C and a series of chemical reactions take place.

There are two major reasons for the poor economic performance of the Fushun-type retorting. First, the remaining retorting gas is not efficiently used but directly burned for

electricity generation.<sup>11</sup> However, the unit heat value of the remaining gas is as low as 3–4 MJ/Nm<sup>3</sup>,<sup>12</sup> so the produced electricity is too little to increase the benefit. In addition, the shale oil is sold at very low price as it contains many impurities.<sup>13,14</sup> Thus, deep processing of shale oil to remove impurities should be applied in the conventional retorting processes. Hydrogenation of shale oil is a common and efficient processing technology to upgrade shale oil to naphtha, diesel, and liquid petroleum gas (LPG). However, the biggest obstacle for hydrogenations is the high price of hydrogen.

Solving the above two problems is important for the development of the oil shale industry. In oil shale mines, there is often a reserve of low-grade coal. For instance, the West Strip Mine in Liaoning province exploits 7 Mt/y oil shale and 2.6 Mt/y coal, while the East Strip Mine exploits 11.9 Mt/y oil shale and 0.8 Mt/y coal (Qian, 2008); the Longkou Mine in Shandong Province exploits 2 Mt/y oil shale and 6 Mt/y lignite. However, the associated coal is often used as thermal coal for heat and electricity generation. In such a case, the economic value obtained is limited. Coal gasification technology has been used for hydrogen production for decades.<sup>5,7</sup> However, the product hydrogen is usually mixed with different impurities. For hydrogen purification, additional separation processes are required. These processes increase the production cost as well as energy consumption.<sup>15</sup> A new developed, coal-based process for hydrogen production was proposed by Guo and his group.<sup>16–18</sup> It is coal gasification in supercritical water technology which uses supercritical water as the gasification reaction medium. Compared to a traditional coal-based process for hydrogen production, this technology features higher hydrogen yield, better coal adaptability, and easier CO<sub>2</sub> emission reduction.<sup>18,19</sup> It is in quick development,

**Received:** June 17, 2014

**Revised:** November 25, 2014

**Accepted:** December 5, 2014

**Published:** December 5, 2014

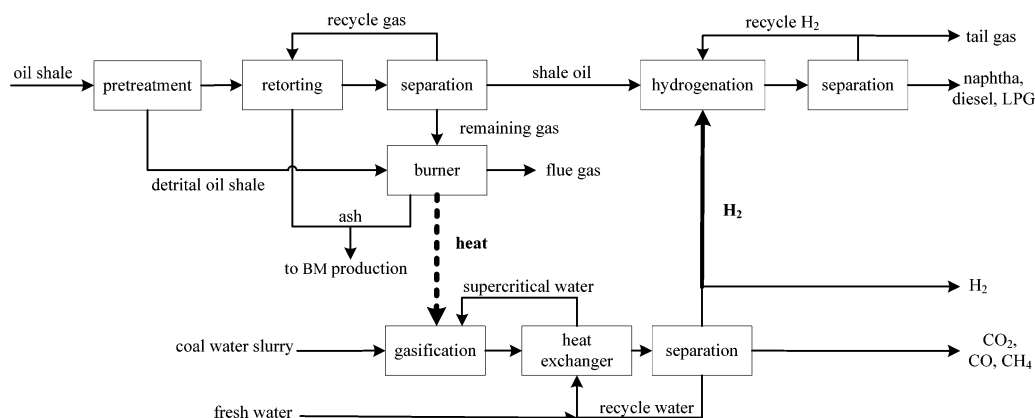


Figure 2. Schematic diagram of the OSR-CGH process.

Table 1. Proximate and Ultimate Analysis of Oil Shale and Lignite

|           | proximate analysis (wt %, ar) |       |       |       | ultimate analysis (wt %, ar) |      |       |      |      |
|-----------|-------------------------------|-------|-------|-------|------------------------------|------|-------|------|------|
|           | M                             | FC    | V     | A     | C                            | H    | O     | N    | S    |
| oil shale | 5.00                          | 3.69  | 18.56 | 72.79 | 79.07                        | 9.93 | 7.02  | 2.12 | 1.86 |
| lignite   | 18.42                         | 15.64 | 32.21 | 33.73 | 61.42                        | 4.93 | 15.30 | 0.86 | 0.29 |

and a demonstration plant has been built in Ningxia Province with the handling capacity of 1.03 t/h lignite.<sup>18</sup> Its hydrogen production can be up to 97.79 kg/h. The demonstration plant verifies the feasibility of large-scale application of the coal gasification in supercritical water technology.

This paper proposes an integrated oil shale refinery process with coal gasification for hydrogen production. The proposed process is explained as well as its promising strengths over the conventional process. The proposed process is modeled and simulated, along with investigations on key operational parameters. The economic performance of the proposed process is analyzed, and the advantages and disadvantages of the proposed process are analyzed by comparing with the oil shale retorting process.

## 2. INTEGRATED OIL SHALE REFINERY PROCESS WITH COAL GASIFICATION

The integrated oil shale refinery process with coal gasification for hydrogen production (OSR-CGH) integrates the coal gasification in supercritical water into the conventional oil shale retorting (OSR) process. It includes an OSR unit, a shale oil hydrogenation (SOH) unit, a coal gasification in supercritical water (CGSW) unit, and a building material production (BMP) unit. The flow sheet of the OSR-CGH process is shown in Figure 2.

After being crushed and screened, oil shale with a diameter of 8–75 mm enters the retort. The oil shale is converted into shale oil, retorting gas, and char at 520 °C. The oil–gas mixture is subsequently separated to obtain shale oil and retorting gas in the separation process. The shale oil enters the shale oil hydrogenation unit to generate high value-added products, naphtha, diesel, and liquid petroleum gas (LPG). The hydrogen used in the hydrogenation unit is provided by the coal gasification in the supercritical water unit.

In the coal gasification, the interphase mass and heat transfer between coal and supercritical water takes place. The organic matter in coal is converted by heterogeneous reactions (liquefaction, pyrolysis, hydrolysis, and extraction) and homogeneous reactions (water gas shift reaction, reforming,

and methanation). Other matter (N, S, As, Hg, etc.) is discharged as inorganic salt. The supercritical water works as the gasification medium to dissolve hydrogen and carbon dioxide. The separation process behind the gasification can easily separate H<sub>2</sub> and CO<sub>2</sub> according to their far different solubilities. High concentration H<sub>2</sub> can be separated by the pressure swing absorption (PSA) process.

Coal gasification in supercritical water is endothermic. Additional heat is needed to drive the reaction. The temperature for this gasification is low and can be provided by waste heat, solar energy, or heat from combustion as Guo et al.<sup>18</sup> suggested. Thus, in the novel process, the waste heat of the retorting gas and the detrital oil shale is enough for the coal gasification in the supercritical water process. Additionally, the hydrogen can be used in the hydrogenation process.

According to the literature by Qian et al.,<sup>5</sup> 325 t/h oil shale approximately produce 12.5 t/h shale oil, emit 50 t/h detrital oil shale and  $4.95 \times 10^4$  Nm<sup>3</sup>/h remaining retorting gas. Their unit heat values are 5.65 MJ/kg and 3.6 MJ/m<sup>3</sup>. They can provide 128.01 MW heat. On the basis of the energy analysis of the coal gasification in the supercritical water process,<sup>18</sup> 2.57 MW is required for the gasification 1 kg lignite in the supercritical state. The hydrogen yield is up to 47.47 mol/kg. This paper assumes that the energy efficiencies of burning detrital oil shale and retorting gas are 70%. The total energy provision is  $128.01 \text{ MW} \times 70\% = 89.61 \text{ MW}$ , which can be used to gasify 34.86 t/h lignite. The gasification could produce 3.31 t/h hydrogen, of which 0.45 t/h hydrogen is used for the 12.5 t/h shale oil hydrogenation process. Even if there is insufficient energy from the detrital oil shale and the remaining retorting gas, additional lignite can be burned to increase combustion temperature or heat.

## 3. MODELING AND SIMULATION OF THE OSR-CGH

For simulation, oil shale and lignite are referred to those in the West Strip Mine in Fushun, Liaoning province, with the proximate and the ultimate analyses shown in Table 1. The amount of input oil shale is  $2.6 \times 10^6$  t/y while that of lignite is  $0.27 \times 10^6$  t/y referring to those in the Fushun. Assuming that

only 85% oil shale particles are in the required size range, the processing capacity of oil shale is  $2.2 \times 10^6$  t/y.

The OSR-CGH process is modeled in Aspen Plus software. The process model includes an OSR unit, CGSW, SOH unit, and a BMP unit. The SOH unit and the BMP unit are not modeled and simulated in this paper. The mass and the energy balances of these units are referred to the reported industrial data or the simulation in other literature.<sup>5</sup> The modeling and simulation of the OSR unit and the CGSW unit are conducted in our work and will be explained in detail in the following section. The key operational parameters for the simulation are summarized in Table 2.

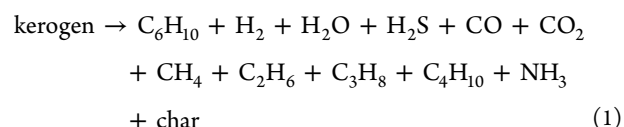
**Table 2.** Key Parameters for the OSR and OSR-CGH Processes Simulation

| key parameters   | value               |
|--|---------------------|
| Oil Shale Retorting Unit                                 |                     |
| retorting temperature, °C                                | 525 <sup>9</sup>    |
| gasification temperature, °C                             | 900 <sup>9</sup>    |
| pressure, MPa  | 0.1 <sup>9</sup>    |
| oil shale flow rate, t/h                                 | 275                 |
| steam rate, t/h  | 60                  |
| air flow rate, t/h                                       | 77                  |
| Coal Gasification in Supercritical Water Unit            |                     |
| reaction temperature, °C                                 | 580 <sup>18</sup>   |
| reaction pressure, MPa                                   | 25 <sup>18</sup>    |
| high pressure, MPa                                       | 25 <sup>21</sup>    |
| low pressure, MPa  | 0.1 <sup>21</sup>   |
| recovery ratio of the PSA process, %                     | 72 <sup>24</sup>    |
| H <sub>2</sub> purity, %                                 | 99.95 <sup>24</sup> |
| minimum temperature difference ( $\Delta T_{\min}$ ), °C | 25 <sup>21</sup>    |
| Shale Oil Hydrogenation Unit                             |                     |
| 1st temperature, °C                                      | 380 <sup>33</sup>   |
| 2nd temperature, °C                                      | 390 <sup>33</sup>   |
| pressure, MPa  | 0.1 <sup>33</sup>   |
| $m(\text{H}_2)/m(\text{shale oil})$                      | 0.03 <sup>33</sup>  |

**3.1. Oil Shale Retorting Process.** In this paper, a Fushun-type retort is selected and modeled. Oil shale is defined as a mixture of water, minerals, and organic matter (kerogen and carbon residues). These components can be separately modeled as mixed, solid, and NC. RK-SOAVE (Redlich–

Kwong–Soave) is selected as the physical property method. The flow sheet of the retorting process is shown in Figure 3.

In the retort, oil shale is converted into shale oil, retorting gas, and char at 0.1 MPa and 525 °C. The retorting process of oil shale retorting is modeled as the continuously stirred tank reactor by the RCSTR model. We defined the holdup of the RCSTR model by valid phase and specification type. The valid phase is assumed as vapor and liquid phases. The specification type is specified by reactor volume and phase volume fraction. In the simulation, we set reactor volume equal to 14.16 dm<sup>3</sup>/t and vapor fraction equal to 0.6. We assume that only organic matter (kerogen) takes part in the decomposition reaction. At high temperature, kerogen is converted into bitumen and then to final products, such as shale oil and hydrocarbon gases. Shale oil is simply formatted as C<sub>6</sub>H<sub>10</sub>. The retorting reaction can be written as



The kinetic equation for the decomposition is as follows:<sup>5,20</sup>

$$\frac{dx}{dt} = k(1 - x)^n \quad (2)$$

where  $x$  is the concentration at a time  $t$ ,  $k$  is the specific rate constant, and  $n$  is the order of the reaction. According to the Arrhenius equation, the expression of the reaction rate constant  $k$  is as follows:

$$k = A e^{-E_a/(RT)} \quad (3)$$

where  $A$  is the apparent frequency factor,  $E_a$  is the apparent activation energy, and  $R$  is the gas constant ( $R = 8.314$  J/mol K). Equation 2 is combined with eq 3 to give eq 4:

$$\frac{dx}{dt} = k(1 - x)^n = A \exp\left(-\frac{E_a}{RT}\right)(1 - x)^n \quad (4)$$

Referring to Qian et al.,<sup>5</sup>  $E_a$  is set to 219.41 kJ/mol,  $A$  is set to  $2.81 \times 10^{13}$ , and  $n$  is 1.0. The kinetic equation of the retorting reaction is converted to

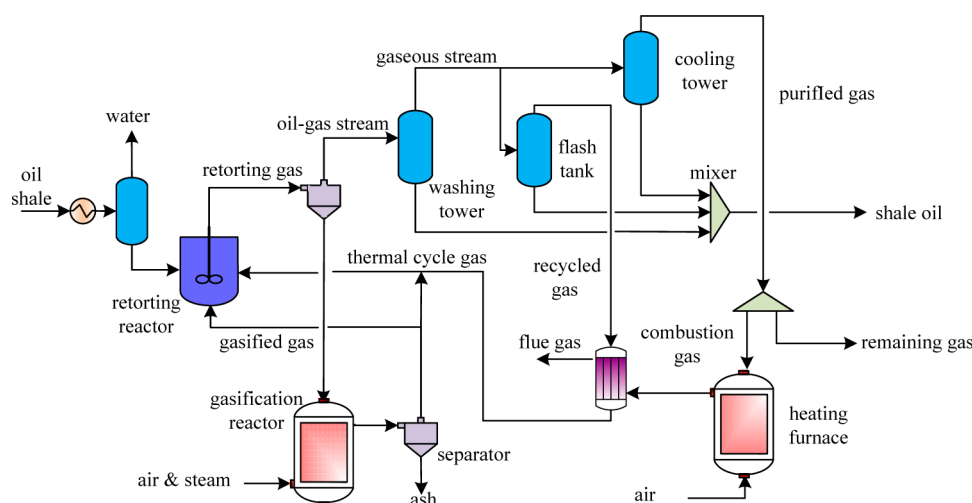


**Figure 3.** Flow diagram of the oil shale retorting process.

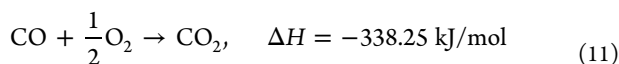
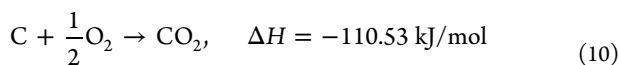
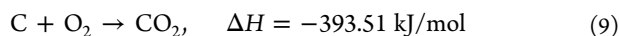
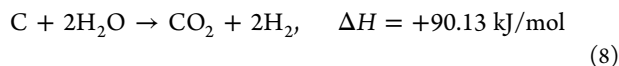
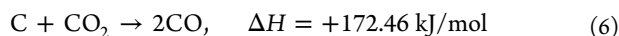
$$\frac{dx}{dt} = k(1-x)^n = 2.81 \times 10^{13} e^{-26.39/T} (1-x) \quad (5)$$

For modeling, the kerogen and the char are defined as nonconventional components. The ultimate analysis of them is shown in Table 3.

**Table 3. Ultimate Analysis of Kerogen and Char**

| elements | ash | C     | H    | N    | Cl | S    | O    |
|----------|-----|-------|------|------|----|------|------|
| kerogen  | 0   | 78.33 | 8.93 | 2.56 | 0  | 3.81 | 6.37 |
| char     | 0   | 81.47 | 0.53 | 6.16 | 0  | 9.23 | 2.61 |

The retorting process is modeled as the combination of the retorting reactor and the gasification reactor. A FORTRAN subroutine is used to control the reaction rate in the retorting reactor. The mixing stream from the retorting reactor consists of shale oil, retorting gas, and char. Char is first separated out in a separator. Then the mixing stream is washed in the washing tower to separate the retorting gas and the shale oil. To get more shale oil, a part of the retorting gas is fed into the flash tank, and the other part is fed into the cooling tower. The gas out of the flash tank as recycle gas is recycled back to the retort. A part of the gas out of the cooling tower is used as fuel gas for the furnace, and the other part is partially fed into the coal gasification unit as feedstock. The solid phase is fed into the gasification reactor at 0.1 MPa and 850 °C. The gasification is modeled by the RGibbs model. It includes a number of reducing reactions (eq 6–8)) and oxidation reactions (eq (8–11)). The outlet stream is then fed into the gas–solid separator to remove ash. The purified gasified gas is recycled to the retorting reactor to provide heat for the retorting reactions.



The simulation results of the oil shale retorting unit are shown in Table 4. The simulation is justified by comparing to industrial data.<sup>5</sup> The relative errors are lower than 3%.

### 3.2. Coal Gasification in Supercritical Water Process.

Referring to the works of Guo et al.,<sup>17,18</sup> the coal gasification in supercritical water is modeled and its flow sheet is shown in Figure 4. SRKMHV2 is selected as the property method.<sup>21</sup> Coal is defined as unconventional solid. Coal gasification process involves coal decomposition and gasification stages. In the

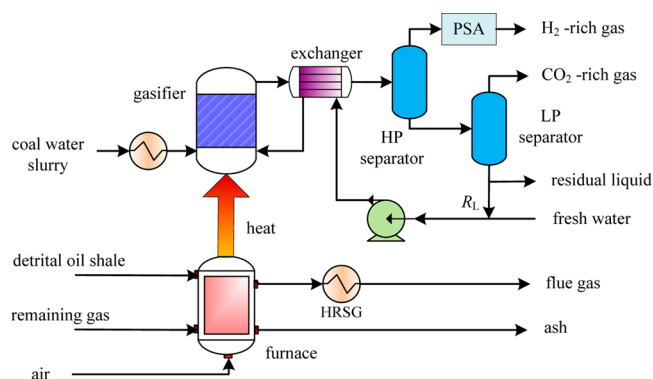
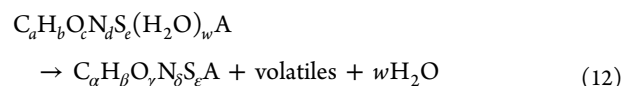
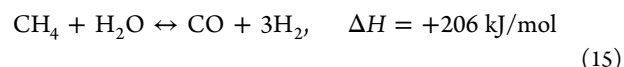


**Figure 4.** Flow diagram of the coal gasification in supercritical water.

decomposition stage, coal ( $C_aH_bO_cN_dS_e(H_2O)_wA$ ) is decomposed into coke, volatiles, and water. Assuming that the coke is simplified to  $C_\alpha H_\beta O_\gamma N_\delta S_\epsilon A$ , the decomposition can be formulated as eq 12.



where A is ash. The composition of coke can be calculated according to the mass balance in eq 12. The decomposition is modeled by the RStoic model. Coal gasification in supercritical water is modeled by the RGibbs model.<sup>22</sup> The gasification process mainly includes three reactions as follows:<sup>18</sup>



The gasification reaction is an endothermic reaction. The heat can be supplied by combustion of the detrital oil shale and the remaining gas which is simulated by the RStoic model. The high-pressure pump raises the pressure and temperature of the feedstock (a mixture of coal and water) to 25 MPa and 580 °C.<sup>23</sup> The product gas from the gasifier is first cooled down by a series of heat exchangers and is then fed into the high-pressure separator to extract  $H_2$ . The  $H_2$  is purified by the PSA process, which is modeled by the ADSIM model. Recovery rate of the PSA process is set to 72% referring to the literature.<sup>24</sup> The high-pressure liquid enters into the low-pressure separator and releases  $CO_2$  in the process of pressure reduction. The residual liquid is mixed with fresh water. The mixture exchanges heat with the product gas. Then it is fed into the gasifier. The heat for the gasification is supplied by the combustion of the detrital oil shale and the retorting gas. For implementation of the new process, the gasification can use a tubular-flow reactor.<sup>18</sup> The detrital oil shale and the remaining gas are burnt in the bottom of a furnace to provide heat for the tubular

**Table 4. Comparison between the Simulation and the Industrial Data of the OSR Unit**

|                              | mole fraction <sup>a</sup> (%) |                |                |      |                 |                 |  | oil productivity (%) |
|------------------------------|--------------------------------|----------------|----------------|------|-----------------|-----------------|--|----------------------|
|                              | N <sub>2</sub>                 | O <sub>2</sub> | H <sub>2</sub> | CO   | CO <sub>2</sub> | CH <sub>4</sub> | C <sub>n</sub> H <sub>m</sub> <sup>b</sup> |                      |
| simulation data              | 54.92                          | 0.40           | 11.91          | 4.55 | 20.79           | 6.70            | 0.73                                       | 6.83                 |
| industrial data <sup>5</sup> | 54.91                          | 0.40           | 11.90          | 4.43 | 20.84           | 6.77            | 0.75                                       | 6.75                 |

<sup>a</sup>Ignore the component with the fraction less than 1 PPM, such as H<sub>2</sub>S and NO. <sup>b</sup>C<sub>n</sub>H<sub>m</sub> includes C<sub>2</sub>H<sub>4</sub>, C<sub>2</sub>H<sub>6</sub>, C<sub>3</sub>H<sub>8</sub>, C<sub>4</sub>H<sub>10</sub>, etc.



flow gasifier. The gasifier is embedded in the middle of the furnace.<sup>18</sup> The residual ash is discharged from the bottom of the furnace.

**3.3. Shale Oil Hydrogenation and BMP Processes.** The hydrogenation process applies the single stage reaction sequenced process (SSRS) as the flow sheet shown in Figure 5, in which the hydrogenation unit consists of a hydrogenation

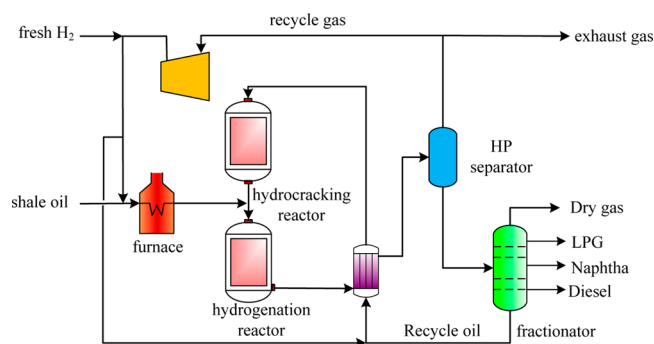


Figure 5. Flow diagram of the hydrogenation process.

reactor and a hydrocracking reactor. Shale oil from the retorting process is heated and mixed with H<sub>2</sub>. The hot stream and the outlet stream from the hydrocracking reactor are sent to the hydrogenation reactor, in which the desulfurization reactions, the denitrogenation reactions, and the hydrogenation reactions take place. The output stream from the hydrogenation reactor is cooled down and then separated to gaseous and liquid phase streams. The separated gaseous stream is recycled back to the hydrogenation reactor, while the liquid stream is refined to diesel, naphtha, and LPG. Oil flows out from the bottom of the fractionator and is mixed with hydrogen and fed into the hydrocracking reactor.

The BMP process uses the ash to make ceramicite and bricks. The simulation of the BMP process refers to the authors' previous work.<sup>9</sup>

**3.4. Analysis of Key Parameters.** Key operational parameters for the proposed process are the retorting temperature, the coal–water slurry concentration, and the recycle ratio of residual liquid ( $R_L$ ). Their effects on the oil productivity and the hydrogen yield are investigated in the following sections.

**Effect of Retorting Temperature.** The retorting temperature is in correlation with the oil and the remaining gas productions as well as the composition of the gas.<sup>25</sup> The remaining gas is burned to provide heat for the coal gasification. The thermal value of the gas, determined by the composition, is important for the energy integration between the retorting process and the coal gasification process.

According to simulation, the production of naphtha, diesel, and LPG rises as the retorting temperature increases, as Figure 6a shows. The increasing rate remains at a high level at the temperature between 400 and 525 °C. This is because the decomposition rate of oil shale increases quickly in this range, leading to the high increase of oil production. However, as the temperature increasing higher than 525 °C, the oil production keeps high but with no obvious increase. This is because only a small amount of the remaining organics can be decomposed in this temperature range. The effect of the retorting temperature on the H<sub>2</sub> and the remaining gas production is shown in Figure 6b. When increasing from 400 to 600 °C, the remaining gas production increases quickly due to the fast decomposition rate

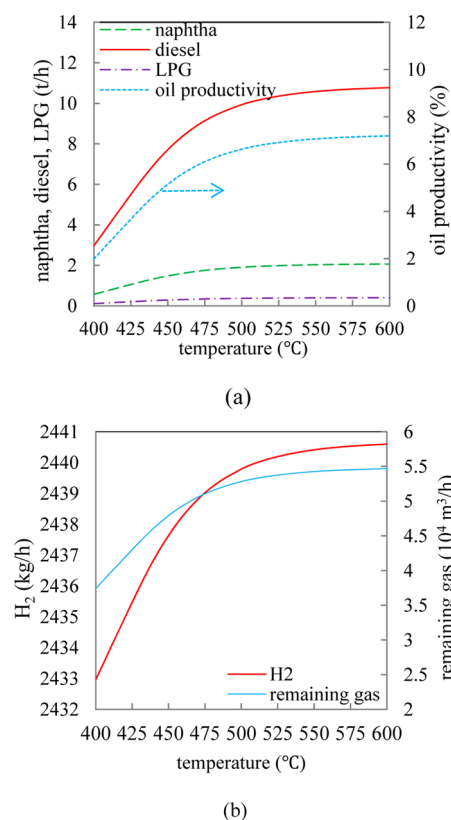


Figure 6. Effect of the retorting temperature on (a) naphtha, diesel, LPG production and oil productivity, (b) H<sub>2</sub> and remaining gas production.

of oil shale. Referring to the work of Yang et al.,<sup>9</sup> the heat value of the remaining gas also increases in this temperature. This increased heat can supply more coal gasification. The hydrogen production therefore increases in this temperature range. As the temperature increases higher than 525 °C, there will be, however, no obvious increase of hydrogen production. According to the above analysis, the operating temperature is set to 525 °C in the following study.

**Effect of Coal–Water Slurry Concentration.** Coal–water slurry concentration affects the production of hydrogen and therefore the economic benefits of the whole OSR-CGH process.<sup>26,27</sup> According to the definition, hydrogen yield ( $Y_{H_2}$ ) is the ratio of moles of hydrogen ( $f_{H_2}$ ) over mass of coal ( $m_{\text{coal}}$ ):<sup>29</sup>

$$Y_{H_2} \% = \frac{f_{H_2}}{m_{\text{coal}}} \times 100 \quad (16)$$

Effect of the concentration is analyzed based on the simulation shows in Figure 7. The yield falls from 28.36 mol/kg to 11.33 mol/kg as the concentration increases from 5% to 20%. Thus, it is found that lower concentration slurry is better for hydrogen production. However, processing the same amount of coal with a lower concentration has to consume more energy than that with a higher concentration. There is a trade-off between effects on the hydrogen production and the energy consumption.

**Effect of Residual Liquid.** The residual liquid from the low pressure separator is recycled back to the gasifier to supplement water in the gasification. The ratio of the recycled liquid over the total liquid out from the low pressure separator is denoted as  $R_L$  as marked in Figure 4. Its effect on the hydrogen yield is

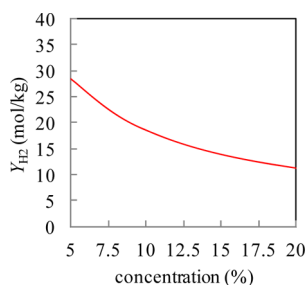


Figure 7. Effect of the slurry concentration on hydrogen yield.

analyzed and shown in Figure 8. As  $R_L$  rises from 0 to 1, the hydrogen yield increases from 25.89 mol/kg to 45.52 mol/kg.

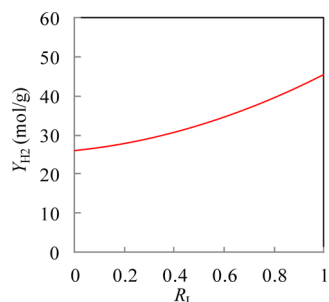


Figure 8. Effect of the recycle ratio on hydrogen yield.

Thus, recycling the residual liquid can increase the chemical conversion in the gasification.

**3.5. Simulation Results.** Based on the parameters study, the retorting temperature is fixed to 525 °C, the slurry concentration is 6 wt %, and the  $R_L$  is 1.0, respectively.

**The OSR Processes.** Referring to the scale of the Fushun retort in Fushun, Liaoning, 275 t/h oil shale processing scale is selected for modeling. This oil shale can produce 12.5 t/h shale oil and  $4.95 \times 10^4$  Nm<sup>3</sup>/h remaining gas. The oil productivity is 6.83% and the oil yield is 66.55%. There are 50 t/h detrital oil shale and 200.17 t/h ashes. On the basis of industrial data,<sup>9</sup> these solid materials could make 36.38 m<sup>3</sup>/h bricks and 10.63 m<sup>3</sup>/h ceramicsite. The mass input and output of the OSR process is shown in Table 5. The utilities consumption (includes stem and electricity) of the OSR process is about 29.4 MW according to the simulation, as shown in Table 6.

Table 5. Main Material Flows of the OSR and OSR-CGH Process

|   | OSR    | OSR-CGH |
|---|--------|---------|
| <b>Input</b>                                      |        |         |
| oil shale (t/h)                                   | 325.00 | 325.00  |
| coal (t/h)  |        | 33.91   |
| <b>Output</b>                                     |        |         |
| shale oil (t/h)                                   | 12.50  |         |
| detrital oil shale (t/h)                          | 50.00  |         |
| naphtha (t/h)                                     |        | 1.95    |
| diesel (t/h)                                      |        | 10.16   |
| LPG (t/h)   |        | 0.38    |
| hydrogen (t/h)                                    |        | 1.99    |
| retorting gas (10 <sup>4</sup> m <sup>3</sup> /h) | 4.95   |         |
| ceramsite (m <sup>3</sup> /h)                     | 10.63  | 12.50   |
| brick (m <sup>3</sup> /h)                         | 36.38  | 42.75   |

Table 6. Utilities Consumption of the OSR-CGH Process

| unit | utility      | value (MW) |
|------|--------------|------------|
| OSR  | electricity  | 6.84       |
|      | steam        | 22.56      |
| SOH  | electricity  | 3.30       |
|      | steam        | 0.43       |
|      | heating fuel | 2.61       |
| CGSW | electricity  | 6.62       |
|      | steam        | 1.42       |

**The OSR-CGH Processes.** The detrital oil shale and the remaining gas are burned to heat the gasifier. The mass input and output of the OSR-CGH process is shown in Table 5. According to the simulation, 12.5 t/h shale oil can produce 1.95 t/h naphtha, 10.16 t/h diesels, and 0.38 t/h LPG. The hydrogenation process consumes 0.45 t/h hydrogen. The simulation shows that the gasifier can process 33.91 t/h lignite with a slurry concentration of 6 wt %. The gasification process can produce 2.20 t/h hydrogen. Only 0.45 t/h hydrogen is used for hydrogenation and the remainder is sold as product. The utilities consumption of the OSR-CGH process is shown in Table 6. While the utilities consumption of the OSR-CGH process is about 43.78 MW, it is 1.49 times of that of the OSR process. The utilities consumption of the SOH and the CGWS process units are 6.34 MW and 8.04 MW. The increase of the electricity consumption in the SOH unit is 3.30 MW caused by hydrogen compression and recycles. That is 6.62 MW in CGSW unit caused by added pumps, PSA, and other equipment. Steam consumption of the OSR-CGH process increases by 8.20% compared to that of the OSR process.

The production cost of the OSR-CGH process is higher than that of the OSR process. But the income from hydrogen product makes the overall benefit increase. The detailed analyses of the economic performance will be conducted in the next section.

#### 4. ECONOMIC ANALYSIS OF THE OSR-CGH

The economic performance is analyzed by capital cost, production cost and return on investment, and then compared to those of the OSR process.

**Capital Investment.** Total capital investment (TCI) mainly consists of fixed capital cost and working capital cost. Equipment cost is estimated by the exponential coefficient method as formatted in eq 17.<sup>30</sup>

$$I_2 = I_1 \left( \frac{Q_2}{Q_1} \right)^{sf} \quad (17)$$

where  $I_1$  and  $I_2$  are the reference and the practical equipment investments;  $Q_1$  and  $Q_2$  are the correspondingly scales; and  $sf$  is the production scale factor. In this paper,  $sf$  is set to 0.67 according to the work of Yi et al.<sup>28</sup>

According to eq 17, the reference equipment cost and the scale of the practical one need to be known. The reference equipment costs of different units and their reference scales are shown in Table 7, referring to previous works.<sup>9,31–33</sup> The total equipment cost for the OSR process and the OSR-RGSR process is 0.20 billion CNY and 0.28 billion CNY. The remainder of the parts, such as installation cost, buildings and land cost, engineering and supervision cost, and construction and contractor cost, are calculated on the basis of their reported proportions to the total capital investment,<sup>34,35</sup> as shown in

Table 7. Benchmark Case for Equipment Investments

| unit | benchmark       | ref scale | ref investment (CNY) | ref    |
|------|-----------------|-----------|----------------------|--------|
| OSR  | oil shale input | 300 t/h   | $185.2 \times 10^6$  | 9, 31  |
| CGSW | coal input      | 10 t/h    | $25.5 \times 10^6$   | 18, 32 |
| SOH  | shale oil input | 10 t/h    | $19.5 \times 10^6$   | 33     |
| BMP  | ash input       | 164 t/h   | $14.9 \times 10^6$   | 9      |

Table 8. The working capital cost is usually set to 20% of the total capital cost according to the work of Zhou et al.<sup>36</sup> After

Table 8. Proportions of Components in the Investment

| component                            | range (%) | basis (%) |
|--------------------------------------|-----------|-----------|
| (1) direct investment                |           |           |
| (1.1) equipment                      | 15–40     | 22        |
| (1.2) installation                   | 6–14      | 8         |
| (1.3) instruments and controls       | 2–8       | 5         |
| (1.4) piping                         | 3–20      | 12        |
| (1.5) electrical                     | 2–10      | 6         |
| (1.6) buildings (including services) | 3–18      | 15        |
| (1.7) land                           | 1–2       | 2         |
| (2) indirect investment              |           |           |
| (2.1) engineering and supervision    | 4–21      | 10        |
| (2.2) construction expenses          | 4–16      | 9         |
| (2.3) contractor's fee               | 2–6       | 4         |
| (2.4) contingency                    | 5–15      | 7         |
| (3) fixed capital                    | (1) + (2) | 100       |
| (4) working capital                  | 15–20     | 20        |
| (5) total capital investment         | (3) + (4) | 120       |

the calculation, the total capital costs of the OSR and the OSR-CGH processes are 0.88 billion CNY and 1.24 billion CNY. The breakdown of the total capital costs are shown in Figure 9.

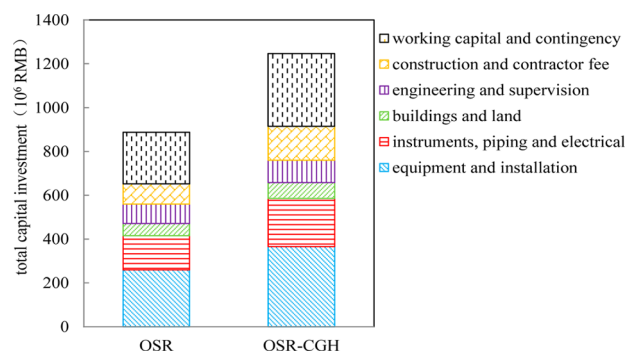


Figure 9. Capital investments of the OSR and OSR-CGH processes.

**Production Cost.** As for the production cost of the OSR and OSR-CGH processes, some assumptions are made and listed in Table 9. In this paper, the cost of raw materials and utilities are calculated according to the simulation described in section 3. The straight-line method<sup>37</sup> was adopted to calculate the depreciation cost under the assumption of 20 years lifetime and 4% salvage value.<sup>38</sup> The remainder of the elements in the production cost are calculated according to their proportion to the total production cost referring to the works of Peters<sup>34</sup> and Orhan.<sup>35</sup> The total production cost (TPC) is defined as the sum of the above components as shown in eq 18:<sup>30</sup>

$$\text{TPC} = C_R + C_U + C_{O\&M} + C_D + C_{POC} + C_{AC} + C_{DSC} \quad (18)$$

Table 9. Assumptions of the Estimation of the Total Production Cost

| component                                   | basis   |
|---|---|
| (1) raw material cost                       | oil shale 55 CNY/t; lignite 300 CNY/t; H <sub>2</sub> 23000 CNY/t                                     |
| (2) utilities cost                          | H <sub>2</sub> O 2.75 CNY/t; electricity 0.65 CNY/kWh; steam 42 CNY/GJ                                |
| (3) operating and maintenance               |   |
| (3.1) operating labor                       | OSR 200 laborers; SOH 80 laborers; CGSW 80 laborers<br>BMP 30 laborers;<br>1 000 000 CNY/laborer/year |
| (3.2) direct supervisory and clerical labor | 20% of operating labor  |
| (3.3) maintenance and repairs               | 2% of fixed capital investment  |
| (3.4) operating supplies                    | 0.8% of fixed capital investment  |
| (3.5) laboratory charge                     | 15% of operating labor  |
| (4) depreciation                            | life period 20 years; salvage value 4%  |
| (5) plant overhead cost                     | 60% (3.1 + 3.2 + 3.3)   |
| (6) administrative cost                     | 2% of product cost  |
| (7) distribution and selling cost           | 2% of product cost  |
| (8) product cost                            | (1) + (2) + (3) + (4) + (5) + (6) + (7)   |

$C_R$  is the raw material cost,  $C_U$  is the utilities cost,  $C_{O\&M}$  is the operating and maintenance cost,  $C_D$  is the depreciation cost,  $C_{POC}$  is the plant overhead cost,  $C_{AC}$  is the administrative cost, and  $C_{DSC}$  is the distribution and selling cost.

After calculation, the total production costs of the OSR and the OSR-CGH processes are 0.46 billion CNY and 0.83 billion CNY. The breakdown is shown in Figure 10. It is found that the production cost of the OSR-CGH process is higher than that of the OSR process.

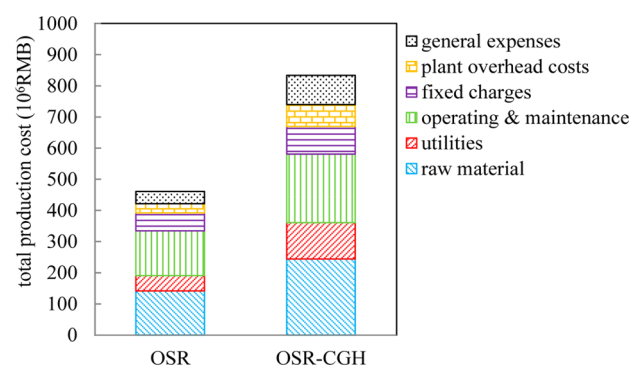


Figure 10. Production costs of the OSR and OSR-CGH processes.

**Return on Investment.** According to the simulation and the prices of products, the total profits of the OSR and the OSR-CGH processes are 170 million CNY/y, and 378 million CNY/y, as shown in Table 10. The economic benefit is reflected by the return on investment (ROI) which is defined as the ratio of the net profit and the total capital investment.<sup>39</sup> According to the above discussion, the ROIs of the two processes are 14.45% and 22.72%, as shown in Figure 11. Thus, the proposed process can create more economic benefit than the OSR process, but requires more capital investment and production cost.



Table 10. Price, Production, and Income of the OSR and OSR-CGH Processes

| item                              | price (CNY) | OSR                |        | OSR-CGH            |         |
|-----------------------------------|-------------|--------------------|--------|--------------------|---------|
|                                   |             | production         | income | production         | income  |
| shale oil (t)                     | 5300        | $10 \times 10^4$   | 530.00 |                    |         |
| naphtha (t)                       | 7100        |                    |        | $1.56 \times 10^4$ | 110.76  |
| diesel (t)                        | 8495        |                    |        | $8.13 \times 10^4$ | 690.64  |
| LPG (t)                           | 6100        |                    |        | $0.30 \times 10^4$ | 18.54   |
| detrital oil shale (t)            | 35.40       | $40.0 \times 10^4$ | 13.45  |                    |         |
| retorting gas (m <sup>3</sup> )   | 0.07        | $3.96 \times 10^8$ | 27.72  |                    |         |
| H <sub>2</sub> (t)                | 23000       |                    |        | $1.40 \times 10^4$ | 322.00  |
| ceramsite (m <sup>3</sup> )       | 160         | $0.85 \times 10^5$ | 12.74  | $1 \times 10^5$    | 14.99   |
| brick (m <sup>3</sup> )           | 175         | $2.91 \times 10^5$ | 46.19  | $3.42 \times 10^5$ | 54.34   |
| total income ( $\times 10^6$ CNY) |             |                    | 630.10 |                    | 1211.27 |
| total profit ( $\times 10^6$ CNY) |             |                    | 170.18 |                    | 377.64  |

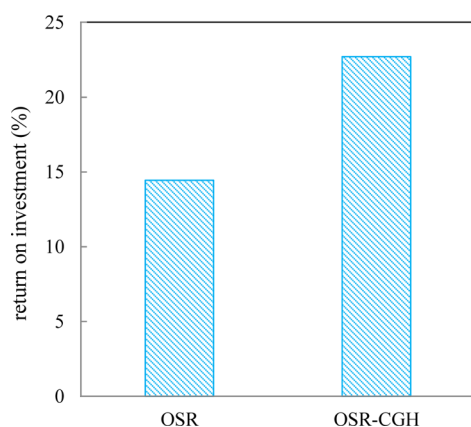


Figure 11. Return on investments of the OSR and OSR-CGH processes.

## 5. CONCLUSIONS

An integrated oil shale refinery process with coal gasification in supercritical water for hydrogen production is proposed in this paper. It integrates the coal gasification process in supercritical water into the conventional oil shale refinery process to produce high-value hydrogen. The hydrogen is produced by the gasification and is partially used in hydrogenation of shale oil. The energy needed for the gasification reaction is provided by the combustion of the detrital oil shale and remaining gas.

The techno-economic analysis of the proposed process is conducted on the basis of the process simulation. The analysis is compared with that of the conventional OSR process. The results show that the proposed process takes more capital cost and production cost because of introduction of the coal gasification unit and the hydrogenation unit. However, the high income of product hydrogen increases the ROI up to 22.72%, much higher than that of the OSR process 14.45%. The proposed process is promising to save the oil shale industry from a low benefit situation, and is worth future study and verification.

## AUTHOR INFORMATION

### Corresponding Author

\*E-mail: cesyyang@scut.edu.cn. Tel.: +86-20-87112056, +86-18588887467.

### Notes

The authors declare no competing financial interest.

## ACKNOWLEDGMENTS

The authors are grateful for financial support from the National Natural Science Foundation of China (Nos. 21136003 and 21306056) and the National Basic Research Program of China (No. 2014CB744306).

## NOMENCLATURE

- $A$  = pre-exponential factor
- $E_a$  = activation energy, kJ/kmol
- $I$  = project investment
- $k$  = reaction rate constants, kmol/m<sup>3</sup>·s·Pa
- $Q$  = production capacity
- $R$  = gas constant, kJ/kmol·K
- $R_L$  = the recycle ratio of liquid residual
- $T$  = temperature, K
- $Y_{H_2}$  = hydrogen yield, mol/kg
- $C_R$  = the raw material cost, CNY/y
- $C_U$  = the utilities cost, CNY/y
- $C_{O\&M}$  = the operating and maintenance cost, CNY/y
- $C_D$  = the depreciation cost, CNY/y
- $C_{POC}$  = the plant overhead cost, CNY/y
- $C_{AC}$  = the administrative cost, CNY/y
- $C_{DSC}$  = the distribution and selling cost, CNY/y

## Abbreviations

- BM = building materials
- BMP = building materials production
- CGSW = coal gasification in supercritical water
- LPG = liquefied petroleum gas
- OSR = oil shale retorting
- OSR-CGH = integrated oil shale refinery with coal gasification for hydrogen production
- PSA = pressure swing absorption
- ROI = return on investment
- SOH = shale oil hydrogenation
- TCI = total capital investment
- TPC = total production cost

## Subscripts

- $n$  = reaction order
- $sf$  = scale factor
- $t$  = time, s
- $x$  = the concentration at a time  $t$ , kg/m<sup>3</sup>

## REFERENCES

- (1) Han, X. X.; Kulaots, I.; Jiang, X. M.; Suuberg, E. M. Review of oil shale semicoke and its combustion utilization. *Fuel* **2014**, *126*, 143–161.

- (2) Li, S. Y. The developments of Chinese oil shale activities. *Oil Shale* **2012**, 29 (2), 101–102.
- (3) Raukas, A.; Siirde, A. New trends in Estonian oil shale industry. *Oil Shale* **2012**, 29 (3), 203–205.
- (4) Guo, H. F.; Si, Y. P.; Jia, D. L.; J, C.; Shan, L.; Tian, B. F.; Yun, Y. L. Retorting oil shale by a self-heating route. *Energy Fuels* **2013**, 27, 2445–2451.
- (5) Qian, J. N.; Yi, L.; Wang, J. Q.; Li, S. Y.; Han, F.; He, Y. G.; . *Oil Shale—Complementary Energy of Petroleum*; China Petrochemical Press: Beijing, 2008 (in Chinese).
- (6) Wang, S.; Jiang, X. M.; Han, X. X.; Tong, J. H. Effect of retorting temperature on product yield and characteristics of non-condensable gases and shale oil obtained by retorting Huadian oil shales. *Fuel Process. Technol.* **2014**, 121, 9–15.
- (7) Li, S. Y.; Tang, X.; He, J. L.; Qian, J. L. Global oil shale development and utilization today—Two Oil Shale Symposiums Held in 2012. *Sino-Global Energy* **2013**, 18 (1), 3–11 (in Chinese).
- (8) Wang, S.; Jiang, X.; Han, X.; Tong, J. H. Investigation of Chinese oil shale resources comprehensive utilization performance. *Energy* **2012**, 42, 224–232.
- (9) Yang, Q. C.; Zhang, J.; Yang, S. Y.; Qian, Y. Modeling and techno-economic analysis of the oil shale comprehensive utilization process. *CIESC J.* **2014**, 65 (7), 2793–2801 (in Chinese).
- (10) Zhang, L. D.; Zhang, X.; Li, S. H.; Wang, Q. Comprehensive Utilization of Oil Shale and Prospect Analysis. *Energy Procedia* **2012**, 17, 39–43.
- (11) Yu, H.; Li, S. Y.; Jin, G. Z. Hydrodesulfurization and hydrodenitrogenation of diesel distillate from Fushun shale oil. *Oil Shale* **2010**, 27 (2), 126–134.
- (12) Yan, F.; Song, Y. Evaluation of Fushun Shale Oil and Study on Processing Project. *Energy Sources* **2008**, 30 (13), 1242–1247.
- (13) Niu, M. T.; Wang, S.; Han, X. X.; Jiang, X. Yield and characteristics of shale oil from the retorting of oil shale and fine oil-shale ash mixtures. *Appl. Energy* **2013**, 111, 234–239.
- (14) Guo, H. F.; Lin, J. D.; Yang, Y. D.; Liu, Y. Y. Effect of minerals on the self-heating retorting of oil shale: Self-heating effect and shale-oil production. *Fuel* **2014**, 118, 186–193.
- (15) Cormos, C. C.; Starr, F.; Tzimas, E.; Peteves, S. Innovative concepts for hydrogen production processes based on coal gasification with CO<sub>2</sub> capture. *Int. J. Hydrogen Energy* **2008**, 33 (4), 1286–1294.
- (16) Li, Y. L.; Guo, L. J.; Zhang, X. M.; Jin, H.; Lu, Y. Hydrogen production from coal gasification in supercritical water with a continuous flowing system. *Int. J. Hydrogen Energy* **2010**, 35 (7), 3036–3045.
- (17) Jin, H.; Lu, Y. J.; Liao, B.; Guo, L. J.; Zhang, X. M. Hydrogen production by coal gasification in supercritical water with a fluidized bed reactor. *Int. J. Hydrogen Energy* **2010**, 35, 7151–7160.
- (18) Guo, L. J.; Jin, H. Boiling coal in water: Hydrogen production and power generation system with zero net CO<sub>2</sub> emission based on coal and supercritical water gasification. *Int. J. Hydrogen Energy* **2013**, 38, 12953–12967.
- (19) Touba, H.; Mansoori, A. Structure and property prediction of sub and supercritical water. *Fluid Phase Equilib.* **1998**, 150–151, 459–468.
- (20) Syed, S.; Qudaih, R.; Talab, I.; Janajreh, I. Kinetics of pyrolysis and combustion of oil shale sample from thermogravimetric data. *Fuel* **2011**, 90 (4), 1631–1637.
- (21) Withag, J. A. M.; Smeets, J. R.; GerritBrem, E. A. B. System model for gasification of biomass model compounds in supercritical water—A thermodynamic analysis. *J. Supercrit. Fluids* **2012**, 61, 157–166.
- (22) Yang, S. Y.; Yang, Q. C.; Man, Y.; Xiang, D.; Qian, Y. Conceptual design and analysis of a nature gas-assisted coal-to-olefins process for CO<sub>2</sub> reuse. *Ind. Eng. Chem. Res.* **2013**, 52 (11), 14406–14414.
- (23) Ge, Z. W.; Guo, S. M.; Guo, L. J.; Cao, C. Q.; Su, X. H.; Jin, H. Hydrogen production by non-catalytic partial oxidation of coal in supercritical water: Explore the way to complete gasification of lignite and bituminous coal. *Int. J. Hydrogen Energy* **2013**, 38, 12786–12794.
- (24) Sircar, S. Applications of gas separation by adsorption for the future. *Adsorpt. Sci. Technol.* **2001**, 19 (5), 347–366.
- (25) Han, X. X.; Jiang, X. M.; Cui, Z. G. Studies of the effect of retorting factors on the yield of shale oil for a new comprehensive utilization technology of oil shale. *Appl. Energy* **2009**, 86 (11), 2381–2385.
- (26) Yu, J.; Yu, J.; Z, L.; Kefa, C. Properties of coal water slurry prepared with the solid and liquid products of hydrothermal dewatering of brown coal. *Ind. Eng. Chem. Res.* **2014**, 53 (11), 4511–4517.
- (27) Kern, S. J.; Pfeifer, C.; Hofbauer, H. Cogasification of polyethylene and lignite in a dual fluidized bed gasifier. *Ind. Eng. Chem. Res.* **2013**, 52 (11), 4360–4371.
- (28) Yi, Q.; Fan, Y.; Li, W. Y.; Feng, J. CO<sub>2</sub> capture and use in a novel coal-based polygeneration system. *Ind. Eng. Chem. Res.* **2013**, 53 (11), 14231–14240.
- (29) Zhang, J.; Weng, X.; Han, Y.; Li, W.; Cheng, J.; Gan, Z.; Gu, J. The effect of supercritical water on coal pyrolysis and hydrogen production: A combined ReaxFF and DFT study. *Fuel* **2013**, 108, 682–690.
- (30) He, C.; You, F. Shale gas processing integrated with ethylene production: Novel process designs, exergy analysis, and techno-economic analysis. *Ind. Eng. Chem. Res.* **2014**, 53 (28), 11442–11459.
- (31) Chen, H. J.; Liu, Z. J.; Zhu, J. W.; Fu, Z. R. Economic evaluation of oil shale utilization. *Geol. Resour.* **2011**, 20 (1), 50–55 (in Chinese).
- (32) Lu, Y.; Zhao, L.; Guo, L. Technical and economic evaluation of solar hydrogen production by supercritical water gasification of biomass in China. *Int. J. Hydrogen Energy* **2011**, 36, 14349–14359.
- (33) Zhao, G. F.; Su, Z. S.; Quan, H. Study on shale oil processing by single-stage reverse sequencing combination hydrocracking-hydro-treating process (FHC-FHT). *Pet. Refin. Eng.* **2012**, 42 (12), 36–38 (in Chinese)..
- (34) Peters, M. S.; Timmerhaus, K. D. *Plant Design and Economics for Chemical Engineers*; McGraw-Hill: New York, 2002.
- (35) Orhan, M. F.; Dincer, I.; Naterer, G. F. Cost analysis of a thermochemical Cu–Cl pilot plant for nuclear-based hydrogen production. *Int. J. Hydrogen Energy* **2008**, 33, 6006–6020.
- (36) Zhou, L.; Chen, W. Y.; Zhang, X. L. Simulation and economic analysis of indirect coal-to-liquid technology coupling carbon capture and storage. *Ind. Eng. Chem. Res.* **2013**, 52, 9871–9878.
- (37) Okoli, C.; Adams, T. A. Design and economic analysis of a thermochemical lignocellulosic biomass-to-butanol process. *Ind. Eng. Chem. Res.* **2014**, 53 (28), 11427–11441.
- (38) Martin, M.; Grossmann, I. E. Optimal simultaneous production of hydrogen and liquid fuels from glycerol: Integrating the use of biodiesel byproducts. *Ind. Eng. Chem. Res.* **2014**, 53 (18), 7730–7745.
- (39) Cho, H. J.; Kim, J. K.; Cho, H. J.; Yeo, Y. K. Techno-economic study of a biodiesel production from palm fatty acid distillate. *Ind. Eng. Chem. Res.* **2013**, 52, 462–468.